Geophys. J. Int. (1996) **127**, 40–48

Ellipticity corrections for seismic phases

B. L. N. Kennett and O. Gudmundsson
Research School of Earth Sciences, The Australian National University, Canberra ACT 0200, *Australia*

Accepted 1996 May 6. Received 1996 February 26

SUMMARY

The advent of broad-band seismology has meant that use is being made of a wide range of seismic phases, for many of which ellipticity corrections have not been readily available. In particular, when many seismic phases are used in location schemes, it is important that the systematic effects of ellipticity are included for each phase.

An efficient and effective procedure for constructing ellipticity corrections is to make use of the ray-based approach of Dziewonksi & Gilbert (1976), as reformulated by Doornbos (1988), in conjunction with the rapid evaluation of traveltimes and slownesses for a given range using the tau-spline procedure of Buland & Chapman (1983).

Ellipticity coefficients have been tabulated for a wide range of seismic phases and are available in electronic form. The ellipticity correction procedures have been extended to include an allowance for diffraction phenomena, for example $P_{\rm diff}$, $S_{\rm diff}$ diffracted along the core–mantle boundary. Corrections for additional phases can be generated by building the ellipticity coefficients from suitable combinations of the coefficients for different phase segments.

Key words: ellipticity corrections, traveltime.

1 INTRODUCTION

As methods for the delineation of the 3-D structure from seismic arrivals have been developed, a wider range of seismic phases have begun to be used. It is important, therefore, that the influence of the ellipticity of the figure of the Earth on seismic traveltimes be taken into account in a comparable way for each seismic phase. The same need arises in the exploitation of later seismic phases in rapid earthquake location using a sparse global array; the systematic effects of ellipticity must be included for all phases used in the location procedure.

The normal model for the calculations of traveltimes for seismic phases is to use a spherical earth with a radial distribution of velocity; aspherical effects are then included via a perturbation treatment. An important component of such asphericity arises from the ellipticity of the figure of the Earth. The resulting influence on the traveltime of a seismic phase will then depend on the location of the source and receiver points, rather than just the epicentral distance Δ between them. For a source at co-latitude ϑ_0, and a path with azimuth ζ to the receiver (measured clockwise from north), Bullen (1937a) introduced triple-entry correction tables $\delta t = \delta t(\vartheta_0, \Delta, \zeta)$ to evaluate the ellipticity correction for P waves; these were later extended to polar latitudes (*cf.* Engdahl & Gunst 1966).

Dziewonski & Gilbert (1976) have developed an elegant representation of the influence of ellipticity on traveltimes and have demonstrated the significance of source depth, z_s, in determining the appropriate corrections. For a seismic phase the correction can be built up from three spherical harmonic components of order 2:

$$\delta t = \sum_{m=0}^{2} \sigma_m(z_s, \Delta) P_{2,m}(\cos \vartheta_0) \cos m\zeta . \tag{1.1}$$

The coefficients $\sigma_m(z_s, \Delta)$ represent ray-path integrals in terms of the radial velocity distribution $v(r)$ as an integral over epicentral distance. Introducing $\lambda_m(\theta)$ as a scaled associated Legendre function,

$$\lambda_m(\theta) = -\frac{2}{3} P_{2,m}(\cos \theta), \tag{1.2}$$

the coefficients $\sigma_m(z_s, \Delta)$ take the form

$$\begin{aligned}\sigma_m(z_s, \Delta) = \frac{1}{p} \int_0^{\Delta} {\rm d}\theta \eta^3(r) \frac{dv}{dr} \varepsilon(r) \lambda_m(\theta) \\ - \sum_j \{\varepsilon \lambda_m(\theta) [(\eta^2 - p^2)^{1/2}]_-^+\}_j \\ \pm \sum_k \{\varepsilon \lambda_m(\theta) [(\eta_\pm^2 - p^2)^{1/2}]_-^+\}_k ,\end{aligned} \tag{1.3}$$

where

$$\eta(r) = v(r)/r , \tag{1.4}$$

p is the ray slowness, $\varepsilon(r)$ is the Earth's ellipticity of figure, and the effect of source depth is implicit in the dependence of r on θ along the ray. The summations represent the influence of discontinuities in velocity (v) in transmission (j) and

reflection (k). Doornbos (1988) has shown how the integrals for $\sigma_m(z_s, \Delta)$ can alternatively be formulated in terms of integrals over radius without sacrificing the convenience of the representation (1.1). Note that the ellipticity coefficients were designated by τ_m by Dziewonski & Gilbert (1976); we have changed to the notation σ_m to avoid conflict with the well-established usage $\tau(p)$ for the delay time, which is also used in Section 2.1.

Dziewonski & Gilbert (1976) presented a tabulation of ellipticity corrections using the $\sigma_m(z_s, \Delta)$ formulation for the phases P, PcP, $PKP_{(ab,bc,df)}$, S, ScS, SKS using the pem model of Dziewonski, Hales & Lapwood (1975). Corrections were given for depths of 0, 300 and 650 km. The perturbations in traveltime are fortunately relatively insensitive to the particular velocity model that is employed. Kennett (1991) extended the $\sigma_m(z_s, \Delta)$ tabulation using the iasp91 model of Kennett & Engdahl (1991) to include a finer tabulation in depth ($z_s = 0$, 35, 50, 10, 200, 300, 500 and 700 km) and additional phases $SKS_{(ac,df)}$, ScP and SKP.

In this paper we demonstrate the convenience of combining the Buland & Chapman (1983) tau-spline procedure for calculating traveltimes, as used by Kennett & Engdahl (1991), with the Doornbos (1988) calculation of the σ_m ellipticity coefficients using ray integrals. An extensive range of ellipticity coefficients have been tabulated and are available in electronic form. The correction procedures have been extended to include an allowance for diffraction phenomena, as for example at the core–mantle boundary in P_{diff}, S_{diff}. Further, we demonstrate how to combine the σ_m coefficients for different phases to produce corrections for cases where the coefficients have not been tabulated.

2 ELLIPTICITY CORRECTIONS

In terms of the $\sigma_m(z_s, \Delta)$ coefficients, the explicit representation of the time correction to be added to the value calculated for a spherically symmetrical earth model is

$$\delta t(z_s, \vartheta_0, \Delta, \zeta) = \frac{1}{4}(1 + 3\cos 2\vartheta_0)\sigma_0(z_s, \Delta) + \frac{\sqrt{3}}{2}\sin 2\vartheta_0 \cos\zeta\sigma_1(z_s, \Delta) + \frac{\sqrt{3}}{2}\sin^2\vartheta_0 \cos 2\zeta\sigma_2(z_s, \Delta), \quad (2.1)$$

where, as before, ϑ_0 is the epicentral co-latitude, Δ is the epicentral distance, ζ is the azimuth from the epicentre to the receiver, and z_s is source depth.

2.1 Ray-based corrections

Doornbos (1988) has presented an effective algorithm for the computation of the σ_m ellipticity coefficients that depends on a specification of the ray parameter for any particular phase. This approach is based on the computation of ray integrals for fixed slowness and in consequence needs to be coupled to an auxiliary routine if corrections are to be produced for fixed epicentral distance, Δ.

Buland & Chapman (1983) have introduced the tau-spline method for rapid construction of traveltimes as explicit functions of range. This method is based on the properties of the delay time τ,

$$\tau(p) = T(p) - p\Delta(p). \quad (2.2)$$

The stationary values of

$$\theta(p, x) = \tau(p) + px = T(p) + p[x - \Delta(p)] \quad (2.3)$$

correspond to geometrical arrivals for the range x. With a tau-spline representation of $\tau(p)$ for each traveltime branch, the condition $\partial\theta(p, x)/\partial p = 0$ leads to the solution of a quadratic to find the slowness, p_x, and then a rapid evaluation of the traveltime for range x from

$$T(x) = \tau(p_x) + p_x x. \quad (2.4)$$

The tau-splines can be established for many phases at a time by using a common-slowness discretization and the superposition of τ segments for different ray segments. The appropriate software has been widely distributed with the release of the iasp91 model (Kennett & Engdahl 1991) and can be readily adapted to different radial velocity models.

The output from the Buland & Chapman (1983) algorithm is ideally suited for use with Doornbos' (1988) ellipticity corrections because the slowness is known explicitly for a given range and phase specification. Thus, provided a ray description is available, the ellipticity coefficients, σ_m, can be calculated rapidly and a cross-check made of the accuracy of the calculation by comparison of the estimated and desired range. For the model ak135 of Kennett, Engdahl & Buland (1995), which is specified by linear gradients in radius, the convergence is better than 0.025° for all the major phases.

This combination of ray algorithms has been used to develop an extensive set of ellipticity corrections in the form of σ_m coefficients as a function of depth, z_s, and range, Δ (see Table 1). These corrections are available in electronic form as detailed in Appendix B.

In the application of such ellipticity corrections, care must be taken where interpolation is applied to ensure that the corrections correspond to the same class of propagation path. It is important to separate the upgoing P and S waves from deep events (P_{up}, S_{up} in Table 1) from the main P and S, which have a separate ray specification.

As noted by Dziewonski & Gilbert (1976) the ellipticity corrections for P and S phases having comparable paths scale very closely with a constant of proportionality that varies from 1.801 to 1.834, i.e. 1.82 ± 0.015, despite the considerable variation in the ratios of P to S wave speed with depth. The constant of proportionality is very close to the value of 1.8 proposed by Bullen (1937b). The simple rescaling works well for mantle phases, such as PcP and ScS, but cannot be applied where the propagation paths have different characters, as for example core phases such as PKP and SKS.

2.2 Diffracted phases

The ellipticity coefficients for a diffracted phase can be determined from the values at the grazing point on the appropriate interface. For a given source depth, z_s, and epicentral distance

Table 1. Ellipticity corrections.

Phase	Δ_{min}	Δ_{max}
P_{up}	0	10
P	5	95
P_{diff}	100	150
PKP_{ab}	145	175
PKP_{bc}	145	155
PKP_{df}	115	180
$PKiKP$	0	155
pP	20	100
$pPKP_{ab}$	145	175
$pPKP_{bc}$	145	155
$pPKP_{df}$	115	180
$pPKiKP$	0	155
sP	5	100
$sPKP_{ab}$	145	175
$sPKP_{bc}$	145	155
$sPKP_{df}$	115	180
$sPKiKP$	0	155
PcP	0	90
ScS	0	60
SKP_{ab}	130	140
SKP_{bc}	130	150
SKP_{df}	110	180
$SKiKP$	0	145
$PKKP_{ab}$	235	255
$PKKP_{bc}$	235	285
$PKKP_{df}$	210	360
$SKKP_{ab}$	215	220
$SKKP_{bc}$	215	280
$SKKP_{df}$	205	360
PP	40	190
$P'P'$	235	360
S_{up}	0	10
S	5	95
S_{diff}	100	150
SKS_{ac}	65	140
SKS_{df}	105	180
pS	60	100
$pSKS_{ac}$	70	140
$pSKS_{df}$	110	180
sS	20	100
$sSKS_{ac}$	65	140
$sSKS_{df}$	110	180
ScS	0	90
PcS	0	60
PKS_{ab}	130	140
PKS_{bc}	130	145
PKS_{df}	110	180
$PKKS_{ab}$	215	220
$PKKS_{bc}$	215	280
$PKKS_{df}$	205	360
$SKKS_{ac}$	65	275
$SKKS_{df}$	200	360
SS	40	190
$S'S'$	130	360
SP	55	135
PS	90	135
PnS	65	90

for the grazing ray, Δ_g, we construct the coefficients for the grazing ray:

$\sigma_0^g(z_s, \Delta_g), \sigma_1^g(z_s, \Delta_g), \sigma_2^g(z_s, \Delta_g)$.

As detailed in Appendix A, the ellipticity coefficients for diffracted waves are specified by two integrals along the upward leg of the grazing ray:

$$X = \frac{1}{p}\int_{\Delta_a}^{\Delta_g} d\theta \cos 2\theta\varepsilon\eta^3 \frac{dv}{dr} - \sum_j \{\varepsilon \cos 2\theta[(\eta^2 - p^2)^{1/2}]_-^+\}_j \pm \sum_k \{\varepsilon \cos 2\theta[(\eta_\pm^2 - p^2)^{1/2}]_-^+\}_k, \quad (2.5)$$

$$Y = \frac{1}{p}\int_{\Delta_a}^{\Delta_g} d\theta \sin 2\theta\varepsilon\eta^3 \frac{dv}{dr} - \sum_j \{\varepsilon \sin 2\theta[(\eta^2 - p^2)^{1/2}]_-^+\}_j \pm \sum_k \{\varepsilon \sin 2\theta[(\eta_\pm^2 - p^2)^{1/2}]_-^+\}_k. \quad (2.6)$$

The change in arc length due to ellipticity is second order in ε and may therefore be ignored.

The σ_m^d coefficients for the diffracted phase may then be constructed from those at grazing, σ_m^g, by

$$\sigma_0^d(z_s, \Delta_g + \delta) = \sigma_0^g(z_s, \Delta_g) + \sin\delta(X \sin\delta + Y \cos\delta), \quad (2.7)$$

$$\sigma_1^d(z_s, \Delta_g + \delta) = \sigma_1^g(z_s, \Delta_g) + \frac{2}{\sqrt{3}} \sin\delta(Y \sin\delta - X \cos\delta), \quad (2.8)$$

$$\sigma_2^d(z_s, \Delta_g + \delta) = \sigma_2^g(z_s, \Delta_g) - \frac{1}{\sqrt{3}} \sin\delta(X \sin\delta + Y \cos\delta), \quad (2.9)$$

where δ is the arc distance of diffraction. Only two numerical integrals need to be evaluated to generate the new coefficients. The integrals X and Y are weakly dependent on source depth through the variation in epicentral distance of the grazing point.

The sets of σ coefficients for P_{diff} and S_{diff} diffracted at the core–mantle boundary are illustrated in Fig. 1 as functions of epicentral distance, together with those for P and S. As we expect, there is a smooth transition from the phase defined by a geometric ray to the diffracted phase. For short diffracted legs a simple extrapolation of the geometric results provides an adequate approximation.

The σ coefficients for P_{diff} and S_{diff} are tabulated in Tables 2 and 3 in comparable form to that employed in Kennett (1991) for P and S.

3 COMBINATION OF ELLIPTICITY CORRECTIONS FOR COMPOSITE PHASES

The form of the ellipticity correction (1.2) is the same for all phases with the coefficients σ_m being the only phase-dependent quantity. Thus, if we can construct the wave path of a particular phase as a combination of two or more elementary phases (e.g. $PKKP$ as a combination of PKP and PcP), we can not only construct the correction for the composite phase from the corrections for the elementary phases, but also construct the σ_m tables for the composite phase by a linear combination of the σ_m tables for the elementary phases. Consider, for example, a surface-reflected phase with two legs, a and b, where the point of reflection lies at Δ_a, so that the two propagation legs are $(0, \Delta_a)$ and (Δ_a, Δ) (see Fig. 2). The corrections could be determined by calculating the coefficients for the Δ_a leg and then introducing an apparent source at the reflection point to build a further correction for the arc length

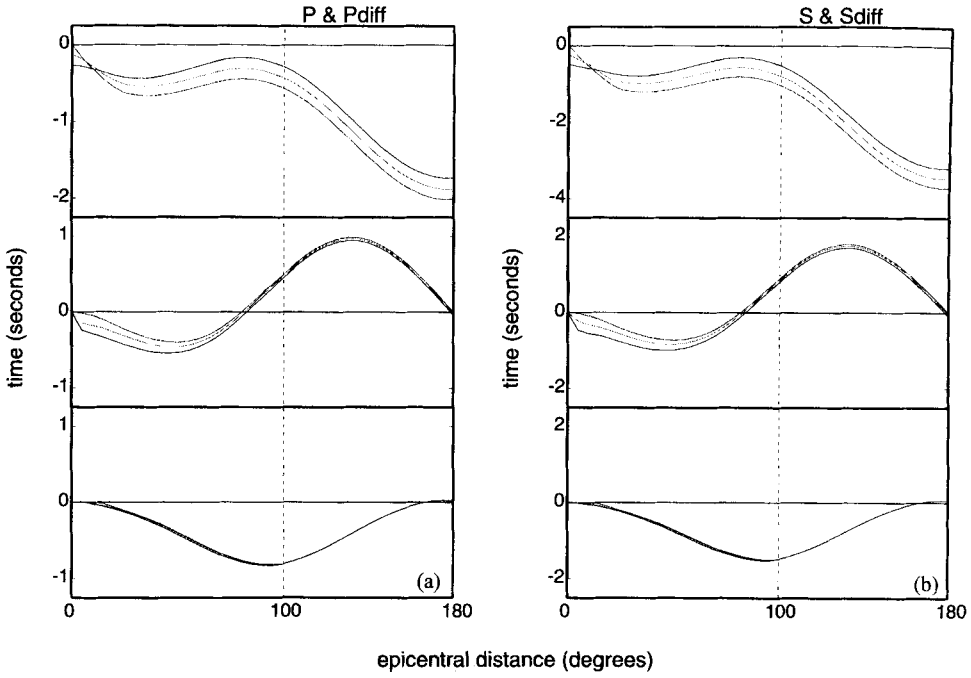

Figure 1. (a) $\sigma_m(\Delta)$ ellipticity coefficients for P and P_{diff}; (b) $\sigma_m(\Delta)$ ellipticity coefficients for S and S_{diff}.

Table 2. Ellipticity coefficients for P_{diff}.

	Depth of source [km]											
	0.			35.			50.			100.		
Δ	σ_0	σ_1	σ_2	σ_0	σ_1	σ_2	σ_0	σ_1	σ_2	σ_0	σ_1	σ_2
100.0	-0.568	0.496	-0.808	-0.550	0.493	-0.808	-0.543	0.492	-0.808	-0.518	0.489	-0.808
105.0	-0.637	0.627	-0.768	-0.620	0.625	-0.768	-0.612	0.623	-0.768	-0.587	0.620	-0.768
110.0	-0.726	0.742	-0.716	-0.708	0.740	-0.717	-0.701	0.739	-0.717	-0.676	0.735	-0.717
115.0	-0.830	0.838	-0.656	-0.813	0.836	-0.656	-0.805	0.835	-0.656	-0.780	0.831	-0.657
120.0	-0.947	0.911	-0.588	-0.930	0.909	-0.589	-0.922	0.908	-0.589	-0.898	0.904	-0.589
125.0	-1.074	0.960	-0.515	-1.056	0.958	-0.516	-1.049	0.957	-0.516	-1.024	0.953	-0.516
130.0	-1.206	0.983	-0.439	-1.188	0.980	-0.439	-1.181	0.979	-0.439	-1.156	0.976	-0.440
135.0	-1.339	0.979	-0.362	-1.322	0.976	-0.362	-1.314	0.975	-0.363	-1.289	0.972	-0.363
140.0	-1.470	0.948	-0.289	-1.452	0.945	-0.287	-1.445	0.944	-0.287	-1.420	0.941	-0.287
145.0	-1.594	0.891	-0.215	-1.576	0.889	-0.215	-1.569	0.888	-0.216	-1.544	0.884	-0.216
150.0	-1.708	0.811	-0.149	-1.690	0.808	-0.150	-1.682	0.807	-0.150	-1.658	0.804	-0.150
	200.			300.			500.			700.		
Δ	σ_0	σ_1	σ_2	σ_0	σ_1	σ_2	σ_0	σ_1	σ_2	σ_0	σ_1	σ_2
100.0	-0.474	0.482	-0.809	-0.431	0.476	-0.809	-0.354	0.465	-0.810	-0.285	0.455	-0.812
105.0	-0.543	0.614	-0.768	-0.501	0.607	-0.769	-0.424	0.596	-0.770	-0.355	0.587	-0.771
110.0	-0.632	0.729	-0.718	-0.590	0.723	-0.718	-0.512	0.711	-0.719	-0.443	0.702	-0.720
115.0	-0.736	0.825	-0.657	-0.694	0.818	-0.658	-0.617	0.807	-0.659	-0.548	0.798	-0.660
120.0	-0.853	0.898	-0.589	-0.811	0.892	-0.590	-0.734	0.881	-0.591	-0.665	0.871	-0.592
125.0	-0.980	0.947	-0.516	-0.938	0.940	-0.517	-0.861	0.929	-0.518	-0.791	0.920	-0.519
130.0	-1.112	0.969	-0.440	-1.070	0.963	-0.441	-0.992	0.952	-0.442	-0.923	0.942	-0.443
135.0	-1.245	0.965	-0.363	-1.203	0.959	-0.364	-1.126	0.948	-0.365	-1.057	0.938	-0.366
140.0	-1.376	0.934	-0.288	-1.334	0.928	-0.288	-1.256	0.917	-0.289	-1.187	0.907	-0.291
145.0	-1.500	0.878	-0.216	-1.458	0.872	-0.217	-1.381	0.860	-0.218	-1.311	0.851	-0.219
150.0	-1.614	0.797	-0.151	-1.572	0.791	-0.151	-1.494	0.780	-0.152	-1.425	0.770	-0.153

Table 3. Ellipticity coefficients for S_{diff}.

	Depth of source [km]											
	0.			35.			50.			100.		
Δ	σ_0	σ_1	σ_2	σ_0	σ_1	σ_2	σ_0	σ_1	σ_2	σ_0	σ_1	σ_2
100.0	-1.041	0.902	-1.480	-1.010	0.896	-1.480	-0.997	0.894	-1.481	-0.953	0.886	-1.481
105.0	-1.167	1.144	-1.407	-1.137	1.138	-1.407	-1.124	1.136	-1.407	-1.080	1.128	-1.407
110.0	-1.329	1.357	-1.314	-1.298	1.351	-1.314	-1.285	1.349	-1.314	-1.241	1.341	-1.314
115.0	-1.520	1.534	-1.204	-1.489	1.529	-1.204	-1.476	1.526	-1.204	-1.432	1.518	-1.204
120.0	-1.734	1.671	-1.080	-1.704	1.665	-1.080	-1.691	1.662	-1.080	-1.647	1.655	-1.080
125.0	-1.966	1.762	-0.946	-1.936	1.756	-0.946	-1.923	1.754	-0.946	-1.879	1.746	-0.946
130.0	-2.208	1.805	-0.806	-2.178	1.799	-0.806	-2.165	1.797	-0.806	-2.121	1.789	-0.806
135.0	-2.453	1.799	-0.664	-2.423	1.794	-0.665	-2.410	1.791	-0.665	-2.366	1.783	-0.665
140.0	-2.694	1.744	-0.526	-2.663	1.739	-0.526	-2.650	1.736	-0.526	-2.606	1.728	-0.526
145.0	-2.922	1.642	-0.394	-2.892	1.636	-0.394	-2.879	1.634	-0.394	-2.835	1.626	-0.394
150.0	-3.132	1.496	-0.273	-3.101	1.490	-0.273	-3.088	1.487	-0.273	-3.044	1.479	-0.273
	200.			300.			500.			700.		
Δ	σ_0	σ_1	σ_2	σ_0	σ_1	σ_2	σ_0	σ_1	σ_2	σ_0	σ_1	σ_2
100.0	-0.876	0.882	-1.482	-0.796	0.860	-1.482	-0.652	0.824	-1.483	-0.528	0.808	-1.484
105.0	-1.003	1.124	-1.408	-0.923	1.102	-1.409	-0.778	1.065	-1.409	-0.655	1.050	-1.411
110.0	-1.165	1.337	-1.315	-1.085	1.314	-1.315	-0.940	1.278	-1.316	-0.816	1.263	-1.318
115.0	-1.356	1.515	-1.205	-1.275	1.492	-1.205	-1.131	1.456	-1.206	-1.007	1.441	-1.207
120.0	-1.570	1.651	-1.081	-1.490	1.628	-1.081	-1.345	1.592	-1.082	-1.222	1.577	-1.084
125.0	-1.802	1.742	-0.947	-1.722	1.719	-0.947	-1.577	1.683	-0.948	-1.454	1.668	-0.950
130.0	-2.045	1.785	-0.807	-1.964	1.763	-0.807	-1.820	1.727	-0.808	-1.696	1.712	-0.810
135.0	-2.289	1.780	-0.666	-2.209	1.757	-0.666	-2.064	1.721	-0.667	-1.941	1.706	-0.668
140.0	-2.530	1.725	-0.527	-2.450	1.702	-0.527	-2.305	1.666	-0.528	-2.181	1.651	-0.530
145.0	-2.758	1.622	-0.395	-2.678	1.600	-0.395	-2.533	1.564	-0.396	-2.410	1.548	-0.398
150.0	-2.968	1.476	-0.274	-2.888	1.453	-0.274	-2.743	1.417	-0.275	-2.619	1.402	-0.277

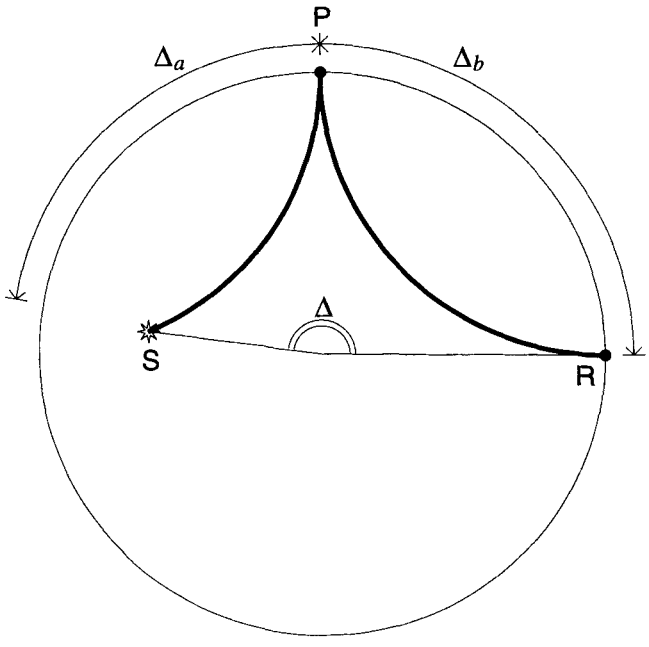

Figure 2. Addition of ray legs to produce a composite phase.

$\Delta_b = \Delta - \Delta_a$. Alternatively, we can use spherical trigonometry to develop an expression for the composite σ_m coefficients:

$$\sigma_0^c(z_s, \Delta) = \sigma_0^a(z_s, \Delta_a) + \frac{1}{2}(3\cos^2\Delta_a - 1)\sigma_0^b(0, \Delta_b) - \frac{\sqrt{3}}{2}\sin 2\Delta_a \sigma_1^b(0, \Delta_b) + \frac{\sqrt{3}}{2}\sin^2\Delta_a \sigma_2^b(0, \Delta_b), \quad (3.1)$$

$$\sigma_1^c(z_s, \Delta) = \sigma_1^a(z_s, \Delta_a) + \frac{\sqrt{3}}{2}\sin 2\Delta_a \sigma_0^b(0, \Delta_b) + \cos 2\Delta_a \sigma_1^b(0, \Delta_b) - \frac{1}{2}\sin 2\Delta_a \sigma_2^b(0, \Delta_b), \quad (3.2)$$

$$\sigma_2^c(z_s, \Delta) = \sigma_2^a(z_s, \Delta_a) + \frac{\sqrt{3}}{2}\sin^2\Delta_a \sigma_0^b(0, \Delta_b) + \frac{1}{2}\sin 2\Delta_a \sigma_1^b(0, \Delta_b) + \frac{1}{2}(1 + \cos^2\Delta_a)\sigma_2^b(0, \Delta_b), \quad (3.3)$$

where

$$\Delta_b = \Delta - \Delta_a . \tag{3.4}$$

The derivation of these expressions is presented in Appendix A.

As a quick check on the composition rules we compared a direct calculation for the coefficients for *PP* at 60°, which is composed of two *P* legs of 30° each, with the results from the application of (3.1)–(3.4). The resulting coefficients differ by no more than 0.006 s, which reflects the truncation errors associated with tabulated values.

More complex combinations of phases can also be made by exploiting the linear superposition of the corrections for different propagation paths. Consider for example, *PKKP*, which can be constructed from the information from *PKP* and *PcP*. For a full propagation path, Δ, we can build the traveltime for *PKKP* by a combination of two *PKP* legs with the subtraction of a *PcP* segment:

$$T^{PKKP}(z_s, \Delta) = T^{PKP}(z_s, \Delta_a) + T^{PKP}(0, \Delta_b) - T^{PcP}(0, \Delta_c), \tag{3.5}$$

where

$$\Delta_c = \Delta_a - (\Delta - \Delta_b). \tag{3.6}$$

Δ_a and Δ_b are the arc lengths of the two *PKP* legs, which have to be found by matching the ray parameter.

The σ_m coefficients for *PKKP* are then found from a linear combination of the coefficients for the *PKP* and *PcP* components:

$$\begin{aligned}\sigma_0^{PKKP}(z_s, \Delta) = {} & \sigma_0^{PKP}(z_s, \Delta_a) + \frac{1}{2}(3\cos^2\Delta_a - 1) \\ & \times [\sigma_0^{PKP}(0, \Delta_b) - \sigma_0^{PcP}(0, \Delta_c)] \\ & - \frac{\sqrt{3}}{2}\sin 2\Delta_a[\sigma_1^{PKP}(0, \Delta_b) - \sigma_1^{PcP}(0, \Delta_c)] \\ & + \frac{\sqrt{3}}{2}\sin^2\Delta_a[\sigma_2^{PKP}(0, \Delta_b) - \sigma_2^{PcP}(0, \Delta_c)],\end{aligned} \tag{3.7}$$

$$\begin{aligned}\sigma_1^{PKKP}(z_s, \Delta) = {} & \sigma_1^{PKP}(z_s, \Delta_a) + \frac{\sqrt{3}}{2}\sin 2\Delta_a\sigma_0^b(0, \Delta_b) \\ & + \cos 2\Delta_a[\sigma_1^{PKP}(0, \Delta_b) - \sigma_1^{PcP}(0, \Delta_c)] \\ & - \frac{1}{2}\sin 2\Delta_a[\sigma_2^{PKP}(0, \Delta_b) - \sigma_2^{PcP}(0, \Delta_c)],\end{aligned} \tag{3.8}$$

$$\begin{aligned}\sigma_2^{PKKP}(z_s, \Delta) = {} & \sigma_2^{PKP}(z_s, \Delta_a) + \frac{\sqrt{3}}{2}\sin^2\Delta_a\sigma_0^b(0, \Delta_b) \\ & + \frac{1}{2}\sin 2\Delta_a[\sigma_1^{PKP}(0, \Delta_b) - \sigma_1^{PcP}(0, \Delta_c)] \\ & + \frac{1}{2}(1 + \cos^2\Delta_a)[\sigma_2^{PKP}(0, \Delta_b) - \sigma_2^{PcP}(0, \Delta_c)].\end{aligned} \tag{3.9}$$

4 DISCUSSION

Although the significance of the Earth's ellipticity on traveltimes has long been recognised, applications have been restricted to a few major phases. The extension of the corrections for diffracted phases and for combinations of seismic phases means that it is now feasible to generate corrections for most observable body-wave phases.

We hope that the provision of a wide range of ellipticity coefficients in readily usable electronic form will encourage the systematic inclusion of the effects of ellipticity in both regional and global studies.

ACKNOWLEDGMENTS

This work was supported in part by grant F49620-94-1-0110 from the US Air Force Office of Scientific Research. We are grateful to the various site managers for the arrangements for ftp access.

REFERENCES

Buland, R. & Chapman, C.H., 1983. The computation of seismic travel times, *Bull. seism. Soc. Am.*, **73**, 1271–1302.

Bullen, K.E., 1937a. The ellipticity correction to travel times of *P* and *S* earthquake waves, *Mon. Not. R. astr. Soc., Geophys. Suppl.*, **4**, 143–157.

Bullen, K.E., 1937b. A suggested new 'seismological' latitude, *Mon. Not. R. astr. Soc., Geophys. Suppl.*, **4**, 158–164.

Doornbos, D.J., 1988. Asphericity and ellipticity corrections, in *Seismological Algorithms*, pp. 75–85, ed. Doornbos, D.J., Academic Press, New York, NY.

Dziewonski, A.M. & Gilbert, F., 1976. The effect of small, aspherical perturbations on travel times and a re-examination of the corrections for ellipticity, *Geophys. J. R. astr. Soc.*, **44**, 7–17.

Dziewonski, A.M., Hales, A.L. & Lapwood, E.R., 1975. Parametrically simple Earth models consistent with geophysical data, *Phys. Earth. planet. Inter.*, **10**, 12–48.

Engdahl, E.R. & Gunst, R.H., 1966. Use of high speed computer for the preliminary determination of earthquake hypocenters, *Bull. seism. Soc. Am.*, **56**, 325–336.

Kennett, B.L.N., 1991. *IASPEI 1991 Seismological Tables*, Research School of Earth Sciences, Australian National University, Canberra.

Kennett, B.L.N. & Engdahl, E.R., 1991. Traveltimes for global earthquake location and phase identification, *Geophys. J. Int.*, **105**, 429–465.

Kennett, B.L.N., Engdahl, E.R. & Buland, R., 1995. Constraints on seismic velocities in the Earth from traveltimes, *Geophys. J. Int.*, **122**, 108–124.

APPENDIX A: CORRECTIONS FOR DIFFRACTED AND COMPOSITE PHASES

A1 Diffracted phases

The geometry of a phase diffracted around a spherical boundary within the Earth is shown and defined in Fig. A1. Energy is radiated downwards from the source at **S** at a particular angle defining a ray parameter, $p = p_g$, such that when the wave refracts towards the boundary it grazes it at point **G**, an arc length Δ_a away from the source. The ray path then refracts upwards towards point **P** on the surface a further arc length Δ_b from **G**. The continuous solid curve in the figure (**SGP**) defines the grazing ray to the boundary. Some energy may diffract along the boundary from **G** to **H**, where it is refracted upwards again to reach the surface at **R**, an arc length $\Delta = \Delta_a + \Delta_b + \delta$ away from the source. At high frequencies the diffracted energy is confined to the upper edge of the boundary and has a predictable traveltime, which is constructed by a path integral of the slowness of the Earth along the path (**SGHR**) shown in Fig. A1, albeit not a 'ray' path. The

geometry of this path and the slowness encountered along it, and consequently the predicted traveltime, will be perturbed by the Earth's ellipticity in a manner much like a true 'ray' path, as formulated by Dziewonski & Gilbert (1976).

We can divide the path **SGHR** (see Fig. A1) into three segments, **SG**, **GH**, and **HR**, and thus construct the perturbation due to ellipticity by combining three contributions. The first and third path segments are 'ray' paths and may be treated as such using the results of Dziewonski & Gilbert (1976). The middle segment, **GH**, encounters a slowness equal to the slowness at the top side of the boundary in the spherical reference earth model used. It therefore suffers no effect other than that due to the change of arc length along the boundary. This in turn is second order in ε, the Earth's ellipticity of figure, and may be ignored. We are then left with the 'ray'-path effects along segments **SG** and **HR**.

Before commencing the derivation from the formulation of Dziewonski & Gilbert (1976), it is convenient to simplify their result (eq. 1.3) by defining

$$f(r) = \frac{1}{p_g}\eta^3(r)\frac{dv}{dr}\varepsilon(r), \tag{A1}$$

and

$$\Delta F_i = -\{\varepsilon[(\eta^2 - p_g^2)^{1/2}]^+_-\}_i \quad \text{or} \quad \Delta F_i = \pm\{\varepsilon[(\eta_\pm^2 - p_g^2)^{1/2}]^+_-\}_i, \tag{A2}$$

depending upon the nature of the interaction with the particular boundary in the Earth, which here is labelled i. We then have a more compact expression for the coefficients σ_m:

$$\sigma_m(z_s, \Delta) = \int_0^\Delta d\theta f(r)\lambda_m(\theta) + \sum_i \Delta F_i \lambda_m(\theta_i). \tag{A3}$$

We can now follow Dziewonski & Gilbert (1976) and write

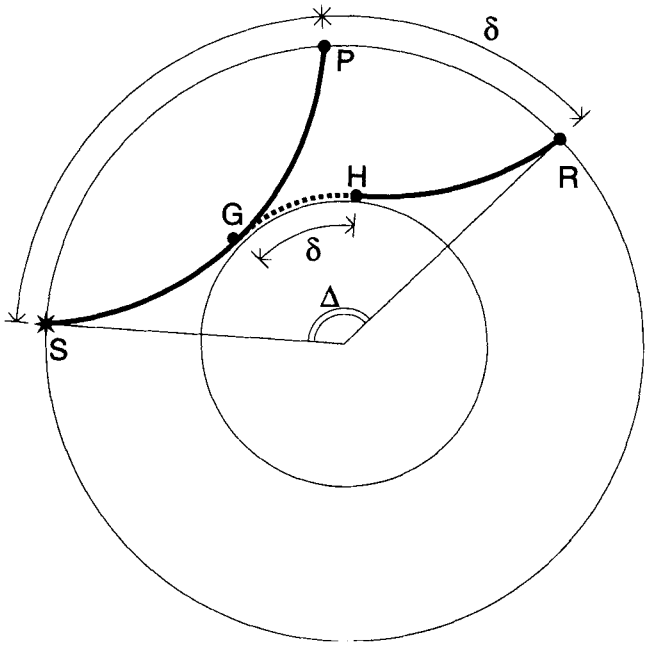

Figure A1. Ellipticity corrections for diffracted phases.

for the diffracted phase

$$\sigma_m^d(z_s, \Delta_g + \delta) = \int_0^{\Delta_a} d\theta f(r)\lambda_m(\theta) + \sum_{i,SG} \Delta F_i \lambda_m(\theta_i) + \int_{\Delta_a}^{\Delta_g} d\theta f(r)\lambda_m(\theta) + \sum_{i,HR} \Delta F_i \lambda_m(\theta_i), \tag{A4}$$

where $\Delta_g = \Delta_a + \Delta_b$ is the epicentral distance of the grazing ray. The sums labelled SG and HR represent sums over all discontinuities in velocity (slowness) encountered by the **SG** and **HR** paths respectively. The θ_i under Σ_{HR} refers to the angular distance from **S** along the **HR** path segment. Note that the **HR** path is a replica of the **GP** path shifted by δ in angular distance from **S**. A simple change of variable in the last two terms of (A4) to $\theta' = \theta - \delta$ thus transforms **HR** to **GP**, and we have

$$\sigma_m^d(z_s, \Delta_g + \delta) = \int_0^{\Delta_a} d\theta f(r)\lambda_m(\theta) + \sum_{i,SG} \Delta F_i \lambda_m(\theta_i) + \int_{\Delta_a}^{\Delta_g} d\theta' f(r)\lambda_m(\theta' + \delta) + \sum_{i,GP} \Delta F_i \lambda_m(\theta_i' + \delta). \tag{A5}$$

Now recall that $\lambda_m(\theta) = -\frac{2}{3}P_{2,m}(\cos\theta)$, where $P_{2,m}$ are associated Legendre functions of degree 2. Simple algebra leads to

$$\begin{aligned}
\lambda_0(\theta + \delta) &= \lambda_0(\theta) + \sin\delta(\sin\delta\cos 2\theta + \cos\delta\sin 2\theta),\\
\lambda_1(\theta + \delta) &= \lambda_1(\theta) + \frac{2}{\sqrt{3}}\sin\delta(\sin\delta\sin 2\theta - \cos\delta\cos 2\theta),\\
\lambda_2(\theta + \delta) &= \lambda_2(\theta) - \frac{1}{\sqrt{3}}\sin\delta(\sin\delta\cos 2\theta + \cos\delta\sin 2\theta).
\end{aligned} \tag{A6}$$

Thus, if we define

$$X = \int_{\Delta_a}^{\Delta_g} d\theta f(r)\cos 2\theta + \sum_{i,GP} \Delta F_i \cos 2\theta_i$$

and

$$Y = \int_{\Delta_a}^{\Delta_g} d\theta f(r)\sin 2\theta + \sum_{i,GP} \Delta F_i \sin 2\theta_i, \tag{A7}$$

we can write

$$\begin{aligned}
\sigma_0^d(z_s, \Delta_g + \delta) &= \int_0^{\Delta_a} d\theta f(r)\lambda_0(\theta) + \sum_{i,SG} \Delta F_i \lambda_0(\theta_i)\\
&\quad + \int_{\Delta_a}^{\Delta_g} d\theta f(r)\lambda_0(\theta) + \sum_{i,GP} \Delta F_i \lambda_0(\theta_i)\\
&\quad + \sin\delta(X\sin\delta + Y\cos\delta)\\
&= \int_0^{\Delta_g} d\theta f(r)\lambda_0(\theta) + \sum_{i,SP} \Delta F_i \lambda_0(\theta_i)\\
&\quad + \sin\delta(X\sin\delta + Y\cos\delta)\\
&= \sigma_0^g(z_s, \Delta_g) + \sin\delta(X\sin\delta + Y\cos\delta),
\end{aligned} \tag{A8}$$

and similarly for σ_1^d and σ_2^d:

$$\sigma_1^d(z_s, \Delta_g + \delta) = \sigma_1^g(z_s, \Delta_g) + \frac{2}{\sqrt{3}}\sin\delta(Y\sin\delta - X\cos\delta), \tag{A9}$$

$$\sigma_2^{\mathrm{d}}(z_{\mathrm{s}}, \Delta_{\mathrm{g}} + \delta) = \sigma_2^{\mathrm{g}}(z_{\mathrm{s}}, \Delta_{\mathrm{g}}) - \frac{1}{\sqrt{3}} \sin \delta (X \sin \delta + Y \cos \delta). \tag{A10}$$

Note that relative to the grazing ray, the change in the σ_m tables is expandable in terms of sin δ, where δ is the arc length of diffraction. Thus, for a short diffraction distance the σ_m tables for the diffracted phase are well represented by a linear extrapolation of the tables for the associated geometrical ray. It is apparent in Fig. 1 that the ellipticity coefficients are continuous to first order across the transition from an optical path to a diffracted path (dashed vertical lines). It is possible to show analytically that this is the case for surface focus paths (S at the surface) and is approximately so in general. The proof of this statement is beyond the scope of this paper. This is potentially useful because if one has the coefficients sufficiently accurately tabulated for the refracted phase one can estimate the integrals X and Y from their derivatives.

It is worth noting that while Fig. A1 draws the diffraction boundary near the core–mantle boundary and our numerical examples are for diffractions around the core–mantle boundary, the arguments and derivation above apply to diffractions around arbitrary spherical boundaries in the Earth. Our derivation holds true whenever the predicted time of the diffracted phase is constructed by a path integral akin to the path depicted in Fig. A1. The derivation applies for example to diffractions off the caustics of upper-mantle triplications.

It is also worth noting that our description of the diffracted path involves a high-frequency assumption. High-frequency diffractions decay rapidly with propagation distance, and the traveltime of diffracted waves is dispersive. The change of traveltime with frequency can be understood in terms of a change in the diffraction geometry. We have not explored the potential deviations from the above derivation due to finite frequency.

A2 Composite phases

If we can construct a wave path of a particular phase as a combination of two or more elementary phases we can evaluate the ellipticity correction for the composite phase by adding the corrections for the elementary phases according to eq. (1.2) using the appropriate epicentral distances, co-latitudes and azimuths. Because the form of the ellipticity corrections is the same for all phases, we can go further and construct the tables of ellipticity coefficients, σ_m, for the composite phase from the σ_m coefficients of the elementary phases. We start by introducing the shorthand

$$g_m(\theta, \zeta) = P_{2,m}(\cos \theta) \cos m\zeta. \tag{A11}$$

We can then write the ellipticity correction for the composite phase, δt^{c}, either in terms of the coefficients for the composite phase, σ_m^{c}, or in terms of the coefficients for the elementary phases, σ_m^{a} and σ_m^{b} (see Fig. A2 for definitions of geometry):

$$\begin{aligned}\delta t^{\mathrm{c}} &= g_0(\theta_{\mathrm{s}}, \zeta_{\mathrm{s}})\sigma_0^{\mathrm{c}}(z_{\mathrm{s}}, \Delta) + g_1(\theta_{\mathrm{s}}, \zeta_{\mathrm{s}})\sigma_1^{\mathrm{c}}(z_{\mathrm{s}}, \Delta) + g_2(\theta_{\mathrm{s}}, \zeta_{\mathrm{s}})\sigma_2^{\mathrm{c}}(z_{\mathrm{s}}, \Delta) \\ &= g_0(\theta_{\mathrm{s}}, \zeta_{\mathrm{s}})\sigma_0^{\mathrm{a}}(z_{\mathrm{s}}, \Delta_{\mathrm{a}}) + g_1(\theta_{\mathrm{s}}, \zeta_{\mathrm{s}})\sigma_1^{\mathrm{a}}(z_{\mathrm{s}}, \Delta_{\mathrm{a}}) \\ &\quad + g_2(\theta_{\mathrm{s}}, \zeta_{\mathrm{s}})\sigma_2^{\mathrm{a}}(z_{\mathrm{s}}, \Delta_{\mathrm{a}}) + g_0(\theta_{\mathrm{p}}, \zeta_{\mathrm{p}})\sigma_0^{\mathrm{b}}(0, \Delta_{\mathrm{b}}) \\ &\quad + g_1(\theta_{\mathrm{p}}, \zeta_{\mathrm{p}})\sigma_1^{\mathrm{b}}(0, \Delta_{\mathrm{b}}) + g_2(\theta_{\mathrm{p}}, \zeta_{\mathrm{p}})\sigma_2^{\mathrm{b}}(0, \Delta_{\mathrm{b}}).\end{aligned} \tag{A12}$$

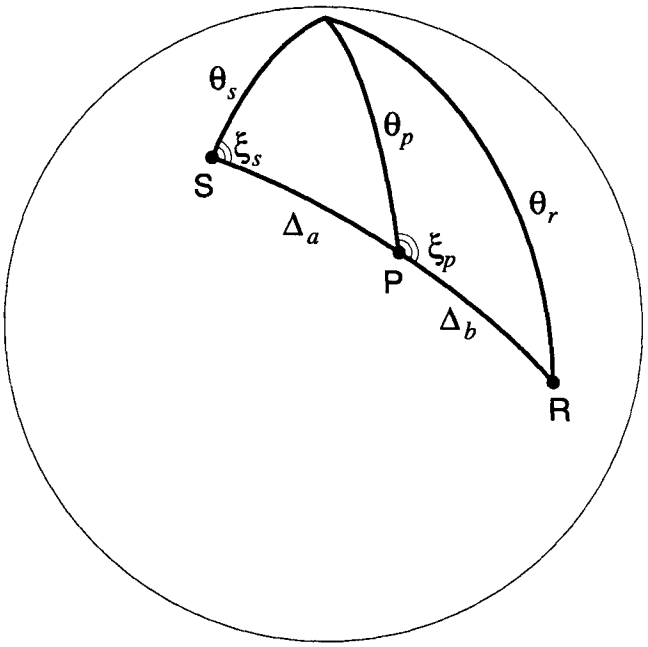

Figure A2. Geometric relations on a sphere for phase addition.

In order to construct the coefficients σ_m^{c} we need to transcribe the terms involving θ_{p} and ζ_{p}, which arise through the shift of the origin of the path for phase b, in terms of θ_{s} and ζ_{s}. We utilize the following relationships from spherical trigonometry (we apply the sine and cosine rules to the left-hand-side triangle in Fig. A2):

$$\sin \zeta_{\mathrm{s}}/\sin \theta_{\mathrm{p}} = \sin(\pi - \zeta_{\mathrm{p}})/\sin \theta_{\mathrm{s}} = \sin \zeta_{\mathrm{p}}/\sin \theta_{\mathrm{s}};$$

$$\cos \theta_{\mathrm{p}} = \cos \theta_{\mathrm{s}} \cos \Delta_{\mathrm{a}} + \sin \theta_{\mathrm{s}} \sin \Delta_{\mathrm{a}} \cos \zeta_{\mathrm{s}};$$

$$\cos \theta_{\mathrm{s}} = \cos \theta_{\mathrm{p}} \cos \Delta_{\mathrm{a}} + \sin \theta_{\mathrm{p}} \sin \Delta_{\mathrm{a}} \cos \zeta_{\mathrm{p}};$$

from which we arrive at

$$\sin \theta_{\mathrm{p}} \sin \zeta_{\mathrm{p}} = \sin \theta_{\mathrm{s}} \sin \zeta_{\mathrm{s}},$$

$$\sin \theta_{\mathrm{p}} \cos \zeta_{\mathrm{p}} = \sin \Delta_{\mathrm{a}} \cos \theta_{\mathrm{s}} - \cos \Delta_{\mathrm{a}} \sin \theta_{\mathrm{s}} \cos \zeta_{\mathrm{s}}$$

by simple algebraic manipulation. We can now rewrite the terms of eq. (A11) that involve θ_{p} and ζ_{p}, the terms $g_m(\theta_{\mathrm{p}}, \zeta_{\mathrm{p}})$, as

$$\begin{aligned}g_0(\theta_{\mathrm{p}}, \zeta_{\mathrm{p}}) &= \frac{1}{4}(1 + 3 \cos 2\Delta_{\mathrm{a}}) g_0(\theta_{\mathrm{s}}, \zeta_{\mathrm{s}}) \\ &\quad + \frac{\sqrt{3}}{2} \sin 2\Delta_{\mathrm{a}} g_1(\theta_{\mathrm{s}}, \zeta_{\mathrm{s}}) + \frac{\sqrt{3}}{2} \sin^2 \Delta_{\mathrm{a}} g_2(\theta_{\mathrm{s}}, \zeta_{\mathrm{s}}), \\ g_1(\theta_{\mathrm{p}}, \zeta_{\mathrm{p}}) &= -\frac{\sqrt{3}}{2} \sin 2\Delta_{\mathrm{a}} g_0(\theta_{\mathrm{s}}, \zeta_{\mathrm{s}}) \\ &\quad + \cos 2\Delta_{\mathrm{a}} g_1(\theta_{\mathrm{s}}, \zeta_{\mathrm{s}}) + \frac{1}{2} \sin 2\Delta_{\mathrm{a}} g_2(\theta_{\mathrm{s}}, \zeta_{\mathrm{s}}), \\ g_2(\theta_{\mathrm{p}}, \zeta_{\mathrm{p}}) &= \frac{\sqrt{3}}{2} \sin^2 \Delta_{\mathrm{a}} g_0(\theta_{\mathrm{s}}, \zeta_{\mathrm{s}}) \\ &\quad - \frac{1}{2} \sin 2\Delta_{\mathrm{a}} g_1(\theta_{\mathrm{s}}, \zeta_{\mathrm{s}}) + \frac{1}{2}(1 + \cos^2 \Delta_{\mathrm{a}}) g_2(\theta_{\mathrm{s}}, \zeta_{\mathrm{s}}).\end{aligned} \tag{A13}$$

We find that they decompose into combinations of terms

$g_m(\theta_s, \zeta_s)$ with weights that depend upon the angular distance of the shift of origin of phase b from that of phase c, Δ_a.

It is now straightforward to match terms in eq. (A11) and write the ellipticity correction coefficients for phase c, σ_m^c, in terms of the coefficients for the elementary phases:

$$\sigma_0^c(z_s, \Delta) = \sigma_0^a(z_s, \Delta_a) + \frac{1}{4}(1 + 3\cos 2\Delta_a)\sigma_0^b(0, \Delta_b) - \frac{\sqrt{3}}{2}\sin 2\Delta_a \sigma_1^b(0, \Delta_b) + \frac{\sqrt{3}}{2}\sin^2 \Delta_a \sigma_2^b(0, \Delta_b),$$

$$\sigma_1^c(z_s, \Delta) = \sigma_1^a(z_s, \Delta_a) + \frac{\sqrt{3}}{2}\sin 2\Delta_a \sigma_0^b(0, \Delta_b) + \cos 2\Delta_a \sigma_1^b(0, \Delta_b) - \frac{1}{2}\sin 2\Delta_a \sigma_2^b(0, \Delta_b),$$

$$\sigma_2^c(z_s, \Delta) = \sigma_2^a(z_s, \Delta_a) + \frac{\sqrt{3}}{2}\sin^2 \Delta_a \sigma_0^b(0, \Delta_b) + \frac{1}{2}\sin 2\Delta_a \sigma_1^b(0, \Delta_b) + \frac{1}{2}(1 + \cos^2 \Delta_a)\sigma_2^b(0, \Delta_b). \quad \text{(A14)}$$

In order to implement these expressions one needs to match the ray parameters of phases a, b, and c in order to determine Δ_a and Δ_b from Δ and then the σ_m tables of phases a and b can be combined to calculate the tables for phase c.

APPENDIX B: ELECTRONIC FORMS FOR ELLIPTICITY CORRECTIONS

A Fortran subroutine ellip provides access to the ellipticity corrections for a given source location, epicentral distance and azimuth using direct access tables of the σ_m coefficients (as specified in Table 1. This subroutine and the necessary direct access table ellipcor.tbl are available using anonymous ftp at the following sites:

(1) the Research School of Earth Sciences, Australian National University, Canberra, Australia: rses.anu.edu.au

(2) the IRIS Data Management Centre in Seattle, Washington, USA: iris.washington.edu

(3) the National Earthquake Information Centre, US Geological Survey, Golden, Colorado, USA: gldfs.cr.usgs.gov, directory ellip

A further program ttimel provides combined access to rapid calculation of seismic traveltimes, using the ak135 model of Kennett *et al.* (1995), with ellipticity corrections for the full range of phases in Table 1.